Available online at www.sciencedirect.com
SCIENCE DIRECT®
Journal of Organometallic Chemistry 689 (2004) 1796–1805
Journal of Organometallic Chemistry
www.elsevier.com/locate/jorganchem

Solution properties, electrochemical behavior and protein interactions of water soluble triosmium carbonyl clusters

Carlo Nervi [a], Roberto Gobetto [a,*], Luciano Milone [a], Alessandra Viale [a], Edward Rosenberg [b,*], Fabrizio Spada [b], Dalia Rokhsana [b], Jan Fiedler [c]

[a] *Dipartimento di Chimica IFM, Universitàdi Torino Via P. Giuria 7, 10125 Torino, Italy*
[b] *Department of Chemistry, University of Montana, Missoula, MT 59812, Bldg. 14, USA*
[c] *J. Heyrovský Institute of Physical Chemistry, Academy of Sciences of the Czech Republic, Dolejškova 3, 18223 Prague, Czech Republic*

Received 23 January 2004; accepted 27 February 2004

Abstract

The synthesis and solution chemistry of the water soluble clusters $[Os_3(CO)_9(\mu\text{-}\eta^2\text{-Bz})(\mu\text{-H})L^+]$ (HBz = quinoxaline, $L^+ = [P(OCH_2CH_2NMe_3)_3I_3]$, **1**) along with its negatively charged analog $[Os_3(CO)_9(\mu\text{-}\eta^2\text{-Bz})(\mu\text{-H})L^-]$ ($L^- = [P(C_6H_4SO_3)_3Na_3]$, **2**) are reported. In addition, we have examined the reduction potentials of the complexes $[Os_3(CO)_9(\mu\text{-}\eta^2\text{-Bz})(\mu\text{-H})L]$ (HBz = phenanthridine, $L = L^+$ (**3**); HBz = 5,6 benzoquinoline, $L = L^+$ (**4**); HBz = 3-amino quinoline, $L = L^+$ (**5**); HBz = 3-amino quinoline, $L = L^-$ (**6**). The neutral analog of **1** and **2** $[Os_3(CO)_9(\mu\text{-}\eta^2\text{-Bz})(\mu\text{-H})\ PPh_3]$ (Bz = quinoxaline, **7**) was also examined for comparison. Both compounds **1** and **2** show pH dependent NMR spectra that are interpreted in terms of the extent of protonation of the uncoordinated quinoxaline nitrogen which impacts the degree of aggregation of the clusters in aqueous solution. Compound **1** undergoes a reversible $1e^-$ reduction in water while **2** undergoes a quasi-reversible $1e^-$ reduction at more negative potentials as expected from the difference in charge on the phosphine ligand. Compound **7** undergoes a marginally reversible CV in methylene chloride at a potential intermediate between the positively and negatively charged clusters. The overall stability of the radical anions of **1, 2** and **7** is somewhat less than the corresponding decacarbonyl $[Os_3(CO)_{10}(\mu\text{-}\eta^2\text{-Bz})(\mu\text{-H})]$ (HBz = quinoxaline). While complexes **1** and **2** show reversible $1e^-$ reductions, all the other complexes examined show $1e^-$ and/or two $1e^-$ irreversible reductions in aqueous and non-aqueous solvents. The potentials for these complexes follow expected trends relating to the charge on the phosphine and the pH of the aqueous solutions. The ligand dependent trends are compared with those of the previously reported corresponding decacarbonyls. The interactions of the positively and negatively charged clusters with albumin have been investigated using the transverse and longitudinal relaxation times of the hydride resonances as probes of binding to the protein. Evidence of binding is observed for both the positive and negative clusters but the positive and negative clusters exhibit distinctly different rotational correlation times. Two additional complexes $[Os_3(CO)_9(\mu\text{-}\eta^2\text{-Bz})(\mu\text{-H})L]$ (HBz = 2-methylbenzimidazole, $L = L^+$ (**8**); $L = L^-$ (**10**) and HBz = quinoline-4-carboxaldehyde, $L = L^+$ (**9**); $L = L^-$ (**11**)) are reported in connection with these studies.

Keywords: Osmium; Clusters; Electrochemistry; Water soluble; Albumin

1. Introduction

Metal complexes have been widely used to elucidate the structure and the function of biological systems [1,2]. In particular, polymetallic complexes can play a singularly active role due to their direct visualization using electron microscopy. Principal handicaps in the use of organometallic carbonyl metal clusters as biological probes are their instability and low solubility in aqueous solutions at physiological pH.

We have developed synthetic procedures for a class of electron deficient complexes of general formula $[Os_3(CO)_9(\mu^3\text{-}\eta^2\text{-Bz})(\mu\text{-H})]$ (HBz = benzoheterocyclic ligand) [3]. Recently, we reported the electrochemical properties of these triosmium clusters where the electron deficiency, according to the effective atomic number

* Corresponding authors. Tel.: +1-406-243-2592; fax: +1-406-243-4227.
E-mail address: rosen@selway.umt.edu (R. Gobetto).

0022-328X/$ - see front matter © 2004 Elsevier B.V. All rights reserved.
doi:10.1016/j.jorganchem.2004.02.036

rule, arises from the presence of a three center two electron bond β to the coordinated pyridinyl nitrogen (Fig. 1) [4]. All of the compounds proved to be electrochemically active but in most of the complexes electrochemically reversible but chemically irreversible reductions were observed. The phenanthridine, 5,6-benzoquinoline electron deficient complexes (Fig. 1) and one electron precise decacarbonyl clusters, $[Os_3(CO)_{10}(\mu\text{-}\eta^2\text{-Bz})(\mu\text{-H})]$ (HBz = quinoxaline) (Eq. (1)) show electrochemically and chemically reversible $1e^-$ reductions. The corresponding stable monoanion radicals have been studied in detail both from the experimental as well as from the theoretical point of view [5,6]. While the LUMO of organometallic clusters is in general localized on the metal core [7], in the case of the clusters mentioned the ligand plays a significant role in the stability of the radical anions. In fact, the LUMO of $[Os_3(CO)_{10}(\mu\text{-}\eta^2\text{-Bz})(\mu\text{-H})]$ (HBz = quinoxaline) is completely centered on the organic ligand.

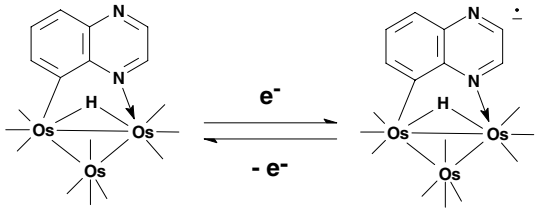

(1)

Most recently, we have become interested in the aqueous chemistry of the complexes illustrated in Fig. 1, modified with water solubilizing ligands. We placed ligands bearing positive $L^+ = [P(OCH_2CH_2NMe_3)_3I_3]$ or negative $L^- = [P(C_6H_4SO_3)Na_3]$ charges on the metal core to provide water solubility. The aromatic ligands in this family of clusters are known intercalators as well as agonists and antagonists for neurotransmitter receptors [1–3]. Recently, we have shown that these clusters, modified with positively charged phosphines, show binding affinities to plasmid DNA that are understandable in terms of the intercalating ability of the ligand bound to the cluster [8]. There are several motivations for developing biomacromolecular labels using polymetallic species containing bioactive ligands besides direct visualization by electron microscopy and the ease with which X-ray phase information can be obtained from diffraction experiments. In addition, it has been pointed out that electrochemically active clusters could combine these features with a sensitive method of detection and/or electron transfer induced cleavage of the biomacromolecules [8,9]. Furthermore, in the case of the clusters reported herein the hydride ligand, which resonates at −10 to −15 ppm, is in a region devoid of all other protons, and represents a potentially useful probe for monitoring cluster binding to biomacromolecules. Therefore, we thought it would be useful to investigate the properties of these water soluble triosmium clusters. We report here the electrochemical behavior of the water soluble clusters and their binding interaction with albumin as probed by the measurement of the spin–lattice and spin–spin relaxation times of the hydride ligand.

2. Experimental

2.1. General

The benzoheterocycle triosmium complexes of general formula $[Os_3(CO)_9(\mu\text{-}\eta^2\text{-Bz})(\mu\text{-H})]$ (HBz = quinoxaline, phenanthridine, 5,6-benzoquinoline, 3-amino- quinoline)

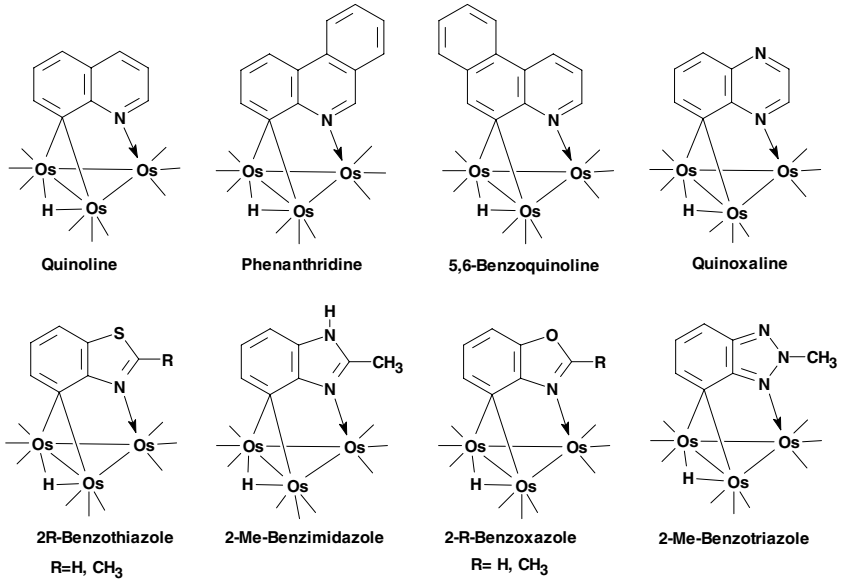

Fig. 1. Structures of the family of electron deficient benzoheterocycle triosmium clusters.

were synthesized according to published procedures [3]. The benzoheterocycle triosmium complex $[Os_3(CO)_9(\mu_3\text{-}\eta^2\text{-Bz})(\mu\text{-H})]$ (HBz = quinoline-4-carboxaldehyde) was prepared according to published literature procedures [6]. The water soluble phosphine derivatives **3**, **5**, **6** and **9** and the positively charged phosphine ligand, $[P(OCH_2CH_2NMe_3)I_3]$, were synthesized according to published literature procedures [8,9]. Osmium carbonyl was purchased from Strem Chemicals and used as received. Sodium triphenylphosphane sulfonate was purchased from Aldrich and used as received.

2.2. Electrochemical measurements

An EG&G Princeton Applied Research Potentionstat/Galvanostat Model M273, connected to a PC with EG&Princeton M270 software, was used. The working electrodes were a dropping mercury electrode (DME) and a glossy carbon electrode (GCE); the reference electrode was a self-made calomel saturated electrode, the counter electrode was a platinum wire. The GCE was polished with wet alumina before use. All solutions used for electrochemical measurements solutions were deoxygenated with an argon purge and were kept under argon flux during the measurements. THF was freshly distilled from benzophenone ketyl and CH_2Cl_2 from phosphorus pentoxide. The pH-measurements were performed with an Amel 334-B pH-meter. Aqueous electrochemical measurements were performed using the following buffer: 0.72 mL of 80% H_3PO_4, 0.57 mL of glacial CH_3COOH, 0.62 g of H_3BO_3 dissolved in water to make 250 mL of stock solution. By adding controlled amounts of 4 M NaOH, pH values between 1.8 and 12.0 can be obtained [10,11]. Electrochemical measurements in organic solvents were done using 0.1 M tetrabutylammonium hexafluorophosphate as the supporting electrolyte. In aqueous solutions, measurements were made against a SCE reference electrode. The non-aqueous reduction potentials are reported with reference to the ferrocene/ferrocenium ion redox couple in the appropriate solvent.

2.3. NMR measurements

The NMR spectra were recorded on Varian Unity Plus 400 MHz, JEOL EX 400 and Bruker Avance 600 MHz spectrometers. The NMR solvents (Aldrich) were dried over activated molecular sieves (Type 4A). Chemical shifts were referenced internally relative to the residual protons in the deuterated solvents used. The 2D NMR measurements were performed using 1024 data points in t_2 and 256 in t_1 with a pulse repetition of 3 s. Non-selective inversion recovery was used to obtain ^1H T_1 values. Samples for T_1 measurements were prepared in the absence of O_2 by using standard freeze–pump–thaw techniques. Temperature calibration was carried out with a methanol standard ^1H thermometer. Errors in the reported T_1 and T_2 values were estimated to be in the range of ±10%. Samples for the experiments with albumin were prepared by dissolving 1 mg (0.001 mmol) of cluster in 0.5 mL of D_2O (no buffer). Precipitation does not occur at any albumin concentration. Clusters used: 3-aminoquinoline negative (**6**); 2-me-benzimidazole negative (**10**); 2-me-benzimidazole positive (**8**); quinoline-4-carboxaldehyde negative (**11**); quinoline-4-carboxaldehyde positive (not completely water soluble) (**9**).

2.4. Synthesis of the water soluble clusters $[Os_3(CO)_9(\mu\text{-}\eta^2\text{-Bz})(\mu\text{-H})(L^+ \text{ or } L^-)]$ (HBz = quinoxaline, L^+ (**1**); L^- (**2**); 5,6-benzoquinoline, L^+ (**4**); 2-methylbenzimidazole, L^+ (**8**); L^- (**10**) and quinoline-4-carboxaldehyde, L^- (**11**) ($L^+ = [P(OCH_2CH_2\ NMe_3)_3I_3]$ $L^- = [P(C_6H_4SO_3)_3Na_3]$)

In a 25 mL round bottom flask 50 mg of $[Os_3(CO)_9(\mu_3\text{-}\eta^2\text{-Bz})(\mu\text{-H})]$ (0.05 mmol) was dissolved in 10 mL of methanol (or acetone), then an equimolar amount of L^+ (38 mg) or L^- (30 mg) dissolved in a few drops of water was added to the cluster solution. The reaction is quantitative and yields 80–88 mg (100%) of yellow to orange product as a precipitate. Analytical and spectroscopic data of the compounds are reported below.

Compound ***1***: Anal. Calc. for $[C_{32}H_{45}N_5O_{12}Os_3PI_3]$: C, 22.7; H, 2.70; N, 4.15. Found: C, 22.01; H, 2.79; N, 3.84%. IR ν(CO) in D_2O: 2094 (m), 2052 (s), 1998 (s), 1937 (sh) cm^{-1}. ^1H NMR in D_2O: δ 9.41 (br, 1H), 8.40 (br, 1H), 8.33 (d, 1H), 7.51 (dd, 2H), 3.40 (m, 6H), 3.07 (s, 3H), 3.04 (s, 3H), 2.90 (s, 27H) and −13.15 (d, 1H, $J_{PH} = 16.47$ Hz).

Compound ***2***: Anal. Calc. for $[C_{35}H_{18}N_2O_{18}Os_3PS_3Na_3]$: C, 27.65; H, 1.85; N, 1.19%. Found: C, 27.03; H, 1.09; N, 1.84. IR (CO) in D_2O: 2089 (sh), 2046 (sh), 1965 (w), 1926 (s) cm^{-1}. ^1H NMR in D_2O: δ 9.47 (s, 1H), 8.22 (s, 1H), 7.73 (d, 1H), 7.60 (m, 6H), 7.2 (s, 6H), 7.03 (d, 1H), 6.75 (s, 1H) and −12.26 (d, 1H, $J_{PH} = 16.09$ Hz).

Compound ***4***: Anal. Calc. for $[C_{37}H_{48}N_4O_{12}Os_3PI_3]$: C, 24.82; H, 2.78; N, 3.23. Found: C, 24.36; H, 2.03; N, 3.25%. IR ν(CO) in D_2O: 2090 (w), 2076 (sh), 2045 (m), 2010 (sh), 1971 (s), 1938 (sh) cm^{-1}. ^1H NMR in D_2O: δ 9.40 (br, 1H), 8.92 (br, 1H), 8.55 (s, 1H), 8.35 (br, 1H), 7.80 (br, 1H), 7.58 (br, 1H), 7.41 (br, 1H), 7.11 (br, 1H), 3.40 (m, 6H), 3.07 (s, 3H), 3.04 (s, 3H), 2.90 (s, 27H) and −13.07 (d, 1H, $J_{PH} = 16.7$ Hz).

Compound ***8***: Anal. Calc. for $[C_{32}H_{46}N_5O_{12}Os_3PI_3]$: C, 22.93; H, 2.74; N, 4.18. Found: C, 22.29; H, 3.60; N, 4.18. IR ν(CO) in D_2O: 2087 (w), 2041 (m), 1997 (s), 1949 (sh) and 1921 (sh) cm^{-1}. ^1H NMR in D_2O: δ 7.40 (t, 1H), 6.90 (d, 1H), 6.80 (d, 1H), 3.40 (m, 6H), 3.07 (s,

3H), 3.04 (s, 3H), 2.90 (s, 27H) and −13.00 (d, 1H, $J_{PH} = 16.88$ Hz).

*Compound **10** (in the hexahydrate form)*: Anal. Calc. for $[C_{35}H_{19}N_2O_{18}Os_3PS_3Na_3]$: C, 26.83; H, 1.99; N, 0.85. Found: C, 26.97; H, 1.99; N, 0.82. IR ν(CO) in D_2O: 2087 (w), 2043 (m), 1998 (s), 1982 (sh) and 1954 (sh) cm^{-1}. ^1H NMR in D_2O: δ 7.60 (t, 1H), 7.50 (d, 1H), 7.40 (m, 12H), 7.20 (d, 1H), 2.40 (s, 3H) and −12.00 (d, 1H, $J_{PH} = 16.37$ Hz).

*Compound **11***: Anal. Calc. for $[C_{37}H_{19}NO_{19}Os_3PS_3Na_3]$: C, 25.84; H, 3.05; N, 3.27. Found: C, 25.76; H, 2.85; N, 3.35%. IR ν(CO) in D_2O: 2088 (w), 2045 (m), 1991 (s), 1955 (sh) and 1926 (sh) cm^{-1}. ^1H NMR in D_2O: δ 9.90 (s, 1H), 9.45 (d, 1H), 8.93 (d, 1H), 7.80 (d, 1H), 7.36(m, 12H), 7.30 (d, 1H), 7.02 (t, 1H) and −12.00 (d, 1H, $J_{PH} = 16.22$ Hz).

2.5. Synthesis of $[Os_3(CO)_9(\mu\text{-}\eta^2\text{-}Bz)(\mu\text{-}H)L]$ (HBz = quinoxaline, L = PPh_3) (7)

In a 25 mL round bottom flask 50 mg of $[Os_3(CO)_9(\mu_3\text{-}\eta^2\text{-}Bz)(\mu\text{-}H)]$ (HBz = quinoxaline, 0.05 mmol) was dissolved in 10 mL methylene chloride then an equimolar amount of PPh_3 (13 mg) was added to the cluster solution. The reaction is quantitative and yields ~60 mg (100%) of red product after evaporation of the solvent and crystallization from CH_2Cl_2–hexane.

*Compound **7***: Anal. Calc. for $[C_{32}H_{21}N_2O_9Os_3P]$: C, 34.57; H, 1.73; N, 2.30. Found: C, 34.38; H, 1.68; N, 2.29%. IR ν(CO) in CH_2Cl_2: 2089 (s), 2048 (s), 2010(s), 1992 (m) 1962 (m) and 1929 (w) cm^{-1} UV/Vis in CH_2Cl_2 (λ_{max}): 395 and 530 nm. ^1H NMR in CD_2Cl_2: δ 9.21 (d, 1H), 8.45 (d, 1H), 7.85 (d, 1H), 7.31 (m, 4H), 7.20(m, 12H), and −11.92 (d, 1H, $J_{PH} = 15.63$ Hz).

3. Results and discussion

3.1. Electrochemical behavior of $[Os_3(CO)_9(\mu\text{-}\eta^2\text{-}Bz)(\mu\text{-}H)(P(OCH_2CH_2NMe_3)_3I_3]$ (**1**, HBz = quinoxaline) in aqueous media

The complex, $[Os_3(CO)_9(\mu\text{-}\eta^2\text{-}Bz)(\mu\text{-}H)(P(OCH_2CH_2NMe_3)_3I_3)]$ (**1**, HBz = quinoxaline, Fig. 2) shows a reversible $1e^-$ reduction. An aqueous solution of **1** (pH 4–5) shows a reversible half-wave potential at −0.62 V vs. SCE at a scan rate of 500 mV/s. The free ligand, quinoxaline, shows irreversible electrochemical behavior on the cyclic voltammetry time scale in both aqueous and non-aqueous media [4,12]. Slight variations in the value of this half-wave potential and the observation of a second partially overlapping wave at more negative potential prompted us to make a more detailed investigation of **1** in aqueous media.

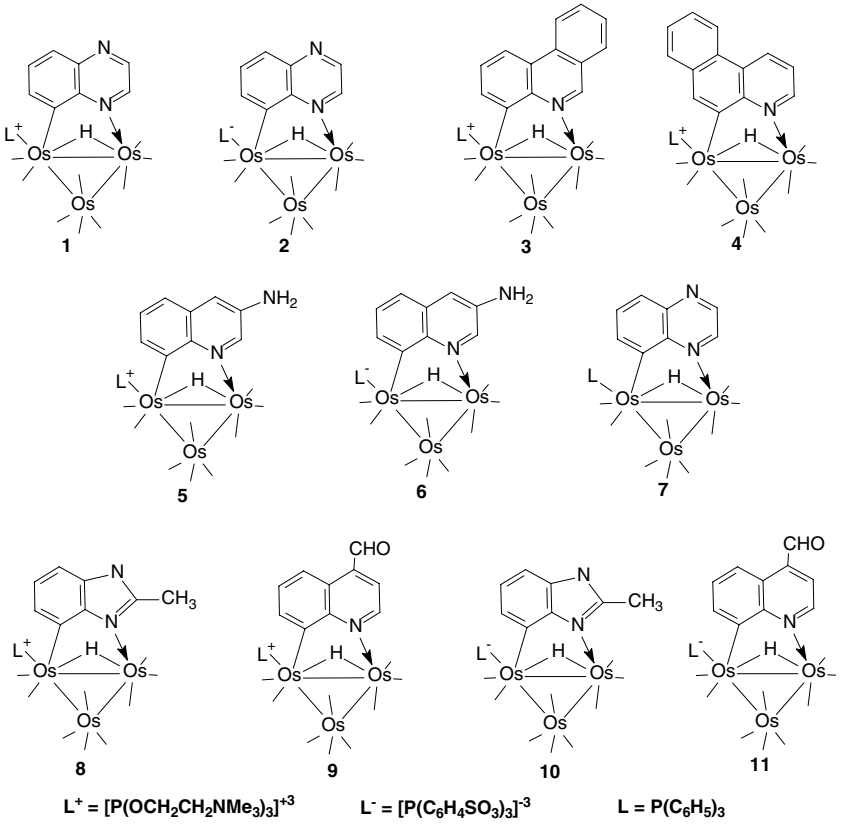

Fig. 2. Structures of the water soluble clusters.

Polarography of **1** in water/0.1 M KCl or phosphate buffer shows two overlapping cathodic waves. Half-wave potentials of both waves are dependent on the pH value, which indicates participation of protonation equilibria in the reduction process. The wave at more positive potential decreases in height on going from acidic to alkaline solution but the overall height of the overlapped waves remains constant up to pH 10. Controlled potential coulometry performed either at the potential of the limiting current plateau of the first wave or at the potential behind the second wave gives approximately the same value of the charge consumption: 1.5 F/mol. Control of the pH can be achieved by means of a $H_3PO_4/CH_3COOH/H_3BO_3$ buffer solution. At pH values lower than 7, CV performed on a glassy carbon (GC) electrode shows that the first reduction at less negative potentials is reversible on the CV time scale (Fig. 3), at scan rates as low as 50 mV/s. The second reduction process overlaps with the first, as the pH values are raised by stepwise addition of a concentrated solution of NaOH (Fig. 4). Also, the intensity of both cathodic peaks is pH dependent, and the decrease in current associated with the first reduction peak correlates with an increase of current for the second reduction peak. This can be easily visualized qualitatively by square wave voltammetry (Fig. 5).

These results lead to the conclusion that the reduction processes in both waves proceed with proton consumption and lead to the same reduction products. This interpretation is supported by polarographic monitoring in non-buffered solutions during electrolysis and formation of hydroxyl ions as detected by the appearance of an anodic wave on the mercury electrode at ca. 0.08 V (vs. SCE). Using a standard addition of NaOH it could be determined that the consumption of one electron results in the formation of one hydroxyl ion [11].

The more positive reduction wave, which is larger in acidic solutions, can be ascribed to the reduction of the protonated complex and the second wave to the reduction of non-protonated species followed by protonation of the reduced form. This is supported by the fact that the aromatic proton resonances of **1** sharpen and show increasing down field shifts as acid is added to a solution of **1** in D_2O. The sharpening is an indication of a decreasing tendency to aggregate as positive charge is placed on the aromatic ring [8]. The hydride signal located at −12.97 ppm is not pH dependent; no other hydride resonance appears during the whole titration ruling out the possibility of a protonation process at the metal triangle. Lowering the pH from 7 to 1.4 results in small downfield shifts for the aromatic resonances with the signal at 9.7 ppm attributable to the proton adjacent to the uncoordinated nitrogen undergoing the largest downfield shift due to aromatic ring protonation at that atom.

That 1.5 F/mol are consumed as observed by coulometry could be the result of competitive follow-up reactions of the reduced, protonated complex; hydrogen evolution with regeneration of the oxidized form of the

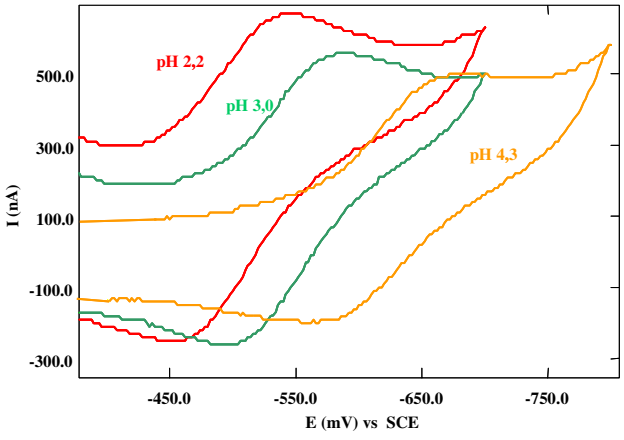

Fig. 3. Cyclic voltammetry of buffered solutions of **1** at 200 mV/s, GC electrode, at values of pH of 2.2, 3.0 and 4.3.

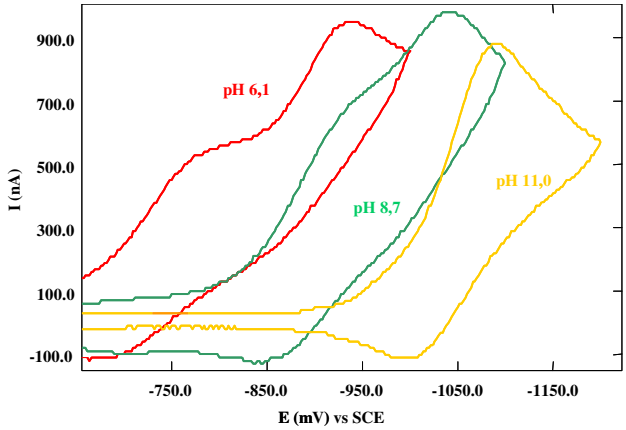

Fig. 4. Cyclic voltammetry of buffered solutions of **1** at 200 mV/s, GC electrode, at values of pH of 6.1, 8.7 and 11.0.

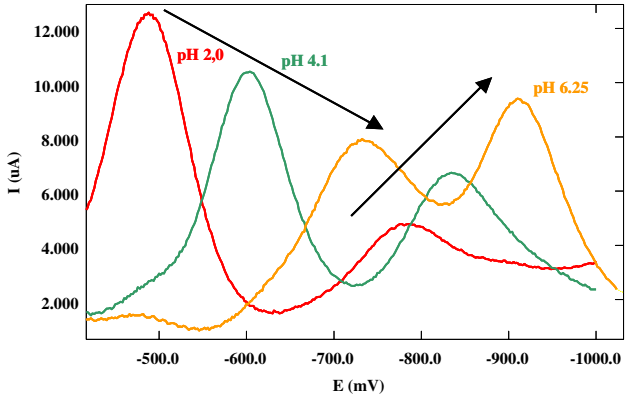

Fig. 5. Square wave voltammetry (SWV) of buffered solutions of **1** at 30 Hz, at values of pH of 2.0, 4.1 and 6.25.

complex and a reaction leading to degradation of the cluster structure.

The pH dependence of the polarographic half-wave potential in the case of the $1e^-$ reduction process ($Ox + 1e^- \rightleftharpoons Red$), with protonation of both oxidized and reduced forms ($Ox + H^+ \rightleftharpoons OxH^+$ and $Red + H^+ \rightleftharpoons RedH^+$), should follow the equation (assuming equal diffusion coefficients) [10,11]

$$E_{1/2} = E_0 + (R/F)\ln(K_a/K'_a) + (RT/F)\ln[(K'_a + [H^+])/(K_a + [H^+])], \quad (1')$$

where K_a, K'_a are the equilibrium dissociation constants of the protonated oxidized and reduced forms, respectively

$$K_a = ([Ox][H^+])/[OxH^+], \quad K'_a = ([Red][H^+])/[RedH^+].$$

Three limiting cases can be considered:

1. In very acid solutions, where $[H^+] \gg K_a, K'_a$, the half-wave potential is independent of pH and is shifted versus standard potential according to relation $E_{1/2} = E_0 + (RT/F)\ln(K_a/K'_a)$.
2. In the pH range $pK_a < pH < pK'_a$, i.e., $K_a \gg [H^+] \gg K'_a$, the equation (1) is simplified to

$$E_{1/2} = E_0 + (RT/F)\ln(K_a/K'_a) + (RT/F)\ln([H^+]/K_a), \quad (2)$$

   i.e., at 25 °C

$$E_{1/2} = E_0 + 0.059\ pK'_a - 0.059\ pH \quad (2')$$

   and a negative potential shift of 59 mV/pH is expected.
3. In alkaline solutions, $[H^+] \ll K_a, K'_a$, the reduction proceeds at the standard potential, $E_{1/2} = E_0$.

The experimentally observed potential shift is linear in the measured range of pH 2–10 and slopes 61 mV/pH are observed. Therefore, from the theoretical relations given the dissociation constants $K_a \sim 10^{-2}$ and $K'_a \sim 10^{-10}$, for oxidized and reduced complex respectively can be estimated (Fig. 6). The plotting of Fig. 6 as an S curve instead of a straight line is based on the calculated values of $E_{1/2}$ at high pH using the above analysis. Unfortunately, it was not possible to check this because of precipitation in the solutions examined above pH 10. In any case, the estimates of K_a and K'_a are taken from the linear region and should be not be significantly impacted by this approximation.

The splitting of the polarographic wave into two overlapping waves and the variation of their heights with pH can be ascribed to an insufficiently mobile equilibrium due to a low value for the rate constant of protonation of the complex in its oxidized form [11].

The cyclic voltammetry measurements are in agreement with the above-proposed mechanism. The reduction in the first wave appears as a reversible cathodic/anodic peak couple. The reoxidation after the cathodic scan going to the second reduction peak proceeds only at the first, more positive wave due to a fast protonation/slow deprotonation of the reduced cluster.

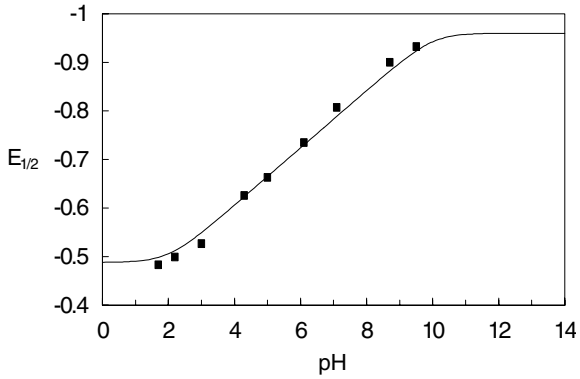

Fig. 6. Dependence of the polarographic half-wave potential of the reduction wave of (**1**) on pH; experimental values (■) and calculated (Eq. (1)) curve for $pK_a = 2$, $pK'_a = 10$.

The polarographic limiting current behind the reduction wave(s) significantly decreases (by ca. 30%) between the pH values 11–12 and the solution color changes from red to green. Obviously, this unknown transformation of the complex stops the side reaction of proton reduction, which increases the polarographic current in more acidic solutions.

*3.2. Electrochemical behavior of [$Os_3(CO)_9(\mu$-η^2-Bz)-(μ-H)(P($OCH_2CH_2NMe_3$)$_3I_3$)] (**1**, HBz = quinoxaline) in non-aqueous media*

In CH_3CN/0.1 M tetrabutylammoniun hexafluorophosphate **1** exhibits two polarographic reduction waves, $E_{1/2} = -1.52$ and -2.01 V (vs. $FeCp_2/FeCp_2^+$), of approximately the same height. The limiting current both behind the first and second wave grows irregularly which indicates formation of decomposition products from the reduced complex. Cyclic voltammetry shows reversibility of the first reduction at higher scan rates (5 V/s). The second reduction appears to be irreversible with only a small anodic counter peak. Coulometry gives $1e^-$/mol for the first wave and after the second $1e^-$ reduction both waves disappear and several new waves of decomposition products appear at more negative potential (which can be reduced with further charge consumption). Reduction directly at the potential behind the second wave gives 2–2.5 F/mol of consumption and a precipitate is formed in the solution. This rather complex electrochemical behavior aside, it is important to note that for complex **1** the initial $1e^-$ reduction gives a more stable reduction product at less negative potentials in aqueous media rather than in non-aqueous media.

3.3. Electrochemical behavior of $[Os_3(CO)_9(\mu\text{-}\eta^2\text{-}Bz)(\mu\text{-}H)(L^+ \text{ or } L^-)]$ (HBz = quinoxaline, L^- (**2**); HBz = phenanthridine, L^+ (**3**); HBz = 5,6-benzoquinoline, L^+, **4**; HBz = 3-NH_2-quinoline, L^+ (**5**); HBz = 3-NH_2-quinoline, L^- (**6**) and the neutral analog $[Os_3(CO)_9(\mu\text{-}\eta^2\text{-}Bz)(\mu\text{-}H)L]$ (HBz = quinoxaline, $L = [P(C_6H_5)_3]$, **7**) ($L^+ = [P(OCH_2CH_2NMe_3)_3I_3]$ and $L^- = [P(C_6H_4SO_3)_3Na_3]$)

The complex **2** in dimethylformamide solution is reduced in a $1e^-$ reversible polarographic wave at −1.74 V (vs. $FeCp_2/FeCp_2^+$). Reversibility was confirmed by cyclic voltammetry and the charge consumption by controlled potential coulometry. In contrast, the complexes **3**–**5** in acetonitrile or dimethylformamide solutions do not exhibit any anodic counter peak on cyclic voltammetry within the range of scan rates employed (0.05–40 V/s), although the corresponding $1e^-$ polarographic waves appear as reversible (**2**) or semi-reversible (slightly decreased slope due to slower electrode reaction; **3**–**5**). This indicates a fast chemical reaction following the charge transfer. Instability of the primary reduction products and a conversion to electro-inactive (non-oxidizable) species is also observed in bulk electrolysis experiments. Reduction of the complex (**6**) is irreversible both in polarography and voltammetry.

The behavior of the complexes **2**–**6** in aqueous solution seems to be analogous in some respects to the behavior of **1**. The polarographic reduction potentials of **2**–**6** in polar organic solvents and in aqueous solution are given in Tables 1 and 2. Two overlapping polarographic waves are shifted to negative potential with increased pH values, thus suggesting a consumption of protons in the reduction process. A reversible electrochemical response is observed only with **2**, at the more positive wave, but only at very fast scan rates. In the case of complexes **3**–**6** the reduction processes are irreversible and furthermore, the waves are ill defined, either obscured by polarographic maxima or overlapping with strongly growing current which possibly originates from hydrogen evolution, catalyzed by the complexes or by decomposition fragments from them. It should be noted that in general the reduction potentials of all the clusters is less negative in water than in non-polar solvents. This is most likely due to the higher dielectric constant and corresponding lower resistivity of the aqueous solutions employed which contained the high salt concentrations required by the buffer system employed. As expected, the positively charged clusters **1** and **5** with the same heterocycle as the negatively charged species **2** and **6** are reduced at less negative potentials. More interestingly, the positively charged clusters **3**–**5** are reduced at more negative potentials than the negatively charged **2** indicating that it is the nature of the heterocycle rather the overall charge on the cluster that determines the reduction potential. This is further corroborated by the electrochemical behavior of the neutral analog, **7**, which shows a reversible $1e^-$ reduction at −1.84V vs. $FeCp_2/FeCp_2^+$ in CH_2Cl_2. As expected the reduction product is less stable than the corresponding decacarbonyl as evidenced by decreasing current of the half-wave with decreasing scan rate. The first reduction potential of **7** is slightly more negative than that of **1** and **2** measured in more polar organic solvents. The limited solubility of **7** in DMF prevented a direct comparison with **1** and **2** but the similarity of the potentials relative to the other complexes certainly supports the idea that the nature of the heterocycle and the substitution of phosphine for CO (i.e. the corresponding decacarbonyl has a reversible wave at −1.16 V in CH_2Cl_2 vs. $FeCp_2/FeCp_2^+$) are the dominant influences on the reduction potential in these complexes rather than the charge on the complex.

Table 1
Polarographic half-wave potential in non-aqueous media, in V vs. $FeCp_2^+/FeCp_2$

Compound	Solvent	$E_{1/2}$	
(**1**)	CH_3CN	−1.52	−2.01
	DMF	−1.56	−2.01
(**2**)	DMF	−1.74	
(**3**)	CH_3CN	−1.89	
(**4**)	CH_3CN	−1.81	
(**5**)	CH_3CN	−1.98	
(**6**)	DMF	−2.24	

Table 2
Polarographic half-wave potential in aqueous media, in V vs. SCE

Compound	pH	$E_{1/2}$	
(**1**)	4.5[a]	−0.62	−0.76
	8.7[a]	−0.85	−0.97
(**2**)	4.5[a]	−0.71	−0.99
	8.7[a]	−0.90	−1.09
(**3**)	4.5[a]	−1.09	−1.51
	8.7[a]	−1.32	−1.78
(**4**)	8.7[a]	−1.45[c]	–[c]
(**5**)	8.7[a]	−1.20[c]	−1.90[c]
(**6**)	–[b]	−1.65[c]	−1.82[c]

[a] Phosphate buffer.
[b] 0.1 M tetrabutylammonium chloride (TBACl).
[c] Ill defined.

3.4. Interaction of the water soluble clusters with albumin

When a 0.001 M solution of the negatively charged cluster $[Os_3(CO)_9(\mu\text{-}\eta^2\text{-}Bz)(\mu\text{-}H)L^-]$ (HBz = 2-methylbenzimidazole, $L^- = [P(C_6H_4SO_3)_3Na_3]$ (**10**)) is titrated with successively increasing amounts of albumin the cluster's ^1H NMR signals progressively broaden. The resonances are detectable until the ratio of albumin/cluster = 0.04, at higher protein concentrations, the signals become too broad to be observed (Fig. 7). Similar behavior is observed for complex **6** and for

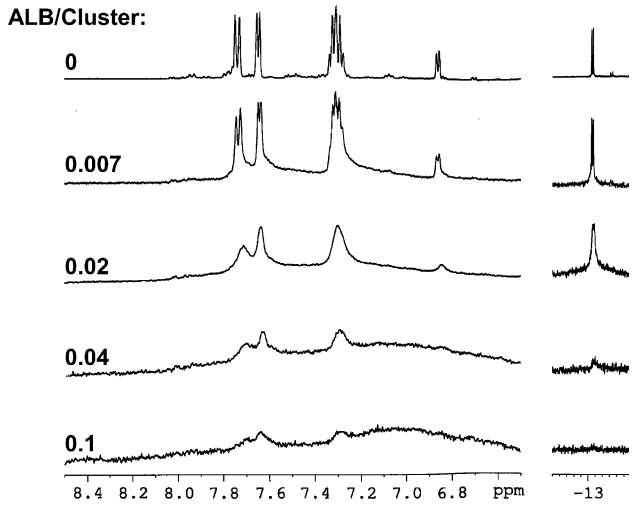

Fig. 7. The ^{1}H NMR spectrum of **10** in the presence of various albumin to cluster ratios measured in water at 600 MHz.

$[Os_3(CO)_9(\mu\text{-}\eta^2\text{-Bz})(\mu\text{-H})\ \ L^-]$ (HBz = quinoline-4-carboxaldehyde, $L^- = [P(C_6H_4SO_3)_3Na_3]$ (**11**)). The latter complex was investigated because it was thought the aldehyde group might covalently attach to the primary amines of the protein and thus show different behavior than the other clusters where only an electrostatic and or π–π stacking interactions are possible. The longitudinal (T_1) and transverse (T_2) relaxation times of the hydride signal before and after the addition of albumin at two different ratios have been measured. The results of these measurements for the three clusters are summarized in Table 3. In all three cases the T_1 increases while the T_2 decreases.

These data can be interpreted in terms of the expected relationship between rotational correlation and the spin lattice relaxation time T_1 (Fig. 8) [13]. According to this relationship there is a minimum value for T_1 that corresponds to a specific rate of molecular rotation where

Table 3
Transverse (T_2) and longitudinal (T_1) relaxation times for the negatively charged clusters $[Os_3(CO)_9(\mu\text{-}\eta^2\text{-Bz})(\mu\text{-H})(P(C_6H_4SO_3)_3Na_3)]$[a,b]

Albumin/cluster	T_1 (s)	T_2 (ms)
*(A) HBz = 2-me-benzimidazole (**10**)*		
0	1.44/1.42	358/383
0.02	2.05/2.14	67/53
0.04	2.03	≅34
*(B) HBz = 3-NH$_2$-quinoline (**6**)*		
0	1.45/1.50	325/704
0.02	1.59/1.47	92/92
0.04	1.74	50
*(C) HBz = quinoline-4-carboxaldehyde (**11**)*		
0	1.52/1.52	641/487
0.02	1.75	200
0.02 after 90°	1.93	120

[a] The two values refer to the two components of the doublet.
[b] Values reported with an error of ±10%.

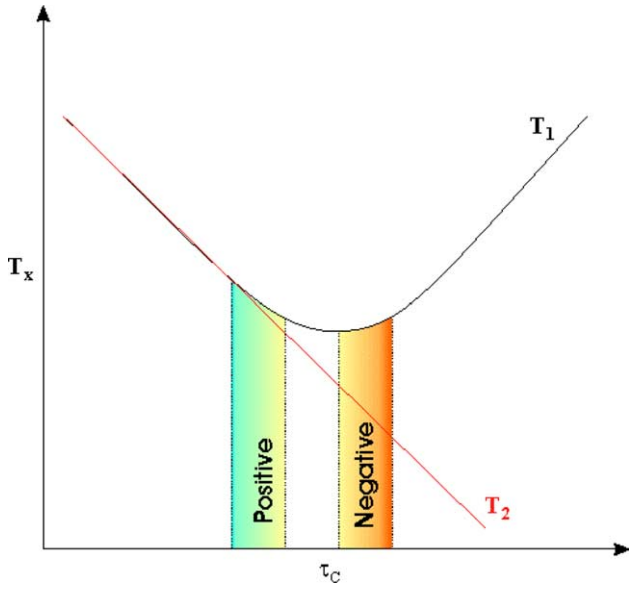

Fig. 8. The relationship between the rotational correlation time and the longitudinal (T_1) and transverse (T_2) relaxation times.

energy transfer is most efficient. Thus, increases in the correlation time τ_c can result in either an increase or a decrease in T_1 depending on whether or not a decrease in the molecular rotation increases the efficiency of energy transfer to the lattice. In the case of the negative clusters **6**, **10** and **11** adduct formation would slow molecular tumbling leading to the conclusion that the correlation is on the positive slope side of the T_1 curve and that therefore the correlation time of the hydride has significantly increased [13]. We do not know what the effect of the phosphine and of the heterocycle on T_1 is, but the relatively large increase in τ_c is consistent with adduct formation. As expected the increase in τ_c is always associated with a decrease in T_2. In the particular case of **11** the albumin cluster solution was heated to 90 °C for 1 h to see if evidence of covalent bonding of the cluster to the protein could be observed [14]. As can be seen from Table 3 there was an increase in T_1 but it is not large enough to attribute irreversible covalent binding of the cluster to the protein [15]. In a separate experiment it was shown that at elevated temperatures **11** isomerizes to a hydride with a different chemical shift and this most likely accounts for the change in T_1.

In order to be sure that the variations observed in the relaxation rates are due to a real interaction with the protein and not simply to the increased viscosity of the solution after albumin addition, the measurements have been repeated on **6** in the presence of different quantities of polyethylene glycol (PEG, M.W. = 1500), which should enhance viscosity presumably without interacting with the cluster. Significantly, no appreciable line broadening of the hydride resonance is observed throughout the concentration range examined and the changes in T_1 and T_2 are relatively small compared with

those observed with albumin (Fig. 9). The vertical line in Fig. 9 represents the concentration ratio where PEG/cluster = 0.04 the value at which maximum yet observable line broadening is seen with albumin. It seems that up to this value (and even for higher concentration), no effect on the relaxation is observed and this means that the variations found in the albumin case are due to the interaction between the cluster and the protein. No significant line broadening of the hydride resonance is observed with the positively charged clusters $[Os_3(CO)_9(\mu\text{-}\eta^2\text{–Bz})(\mu\text{-H})L^+]$ (HBz = 2-me-benzimidazole, $L^+ = [P(OCH_2CH_2NMe_3)_3I_3]$ (**8**); HBz = quinoline-4-carboxaldehyde, $L^+ = [P(OCH_2CH_2NMe_3)_3I_3]$ (**9**)) at albumin/cluster ratios lower than 0.04, while in the negative case broadening is extensive at ratios = 0.02. At ratios of 0.1 the negatively charged cluster hydride resonances in **6**, **10** and **11** are broadened into the base line while in the case of **8** and **9** the hydride resonance is still relatively sharp (Figs. 7 and 10).

The T_1 measurements were carried out on **8** and **9** but at higher albumin concentrations. The results are summarized in Table 4 and it can be seen that here the addition of albumin to the cluster solution results in shorter T_1 values although the T_1 for the cluster itself is not very different than that found for the negative clusters. Considering that there are probably many clusters bound to the albumin at any one time the apparently weaker interaction with the protein would place fewer clusters on the albumin at any one instant leading to more rapid tumbling of the protein and placing this cluster protein system on the negative sloping part of the T_1 curve (Fig. 8). The trend for T_2 is the same found for the negative cluster as expected. The same behavior was observed for **9** as expected (Table 4).

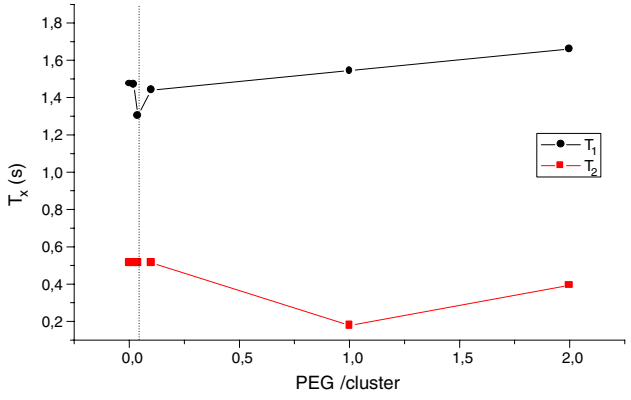

Fig. 9. Plot of the variation in T_1 and T_2 of **6** with added polyethylene glycol (PEG).

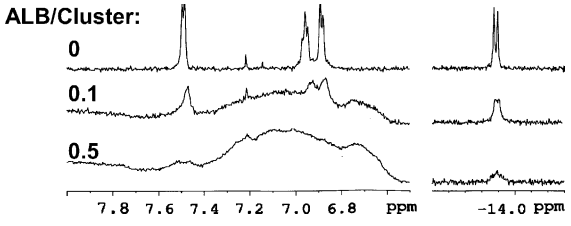

Fig. 10. The ^{1}H NMR spectrum of **8** in the presence of various albumin to cluster ratios measured in water at 600 MHz.

Table 4
Transverse (T_2) and longitudinal (T_1) relaxation times for the positively charged clusters $[Os_3(CO)_9(\mu\text{-}\eta^2\text{-Bz})(\mu\text{-H})(P(C_6H_4SO_3)_3Na_3)]$[a,b]

Albumin/cluster	T_1 (s)	T_2 (ms)
*(A) HBz = 2-me-benzimidazole (**8**)*		
0	1.90/2.07	310/324
0.04	0.77/0.68	53/48
0.1	0.57	≅32
*(B) HBz = quinoline-4-carboxaldehyde (**9**)*		
0	1.93/2.02	312/216
0.02	1.40/1.58	147/98

[a] The two values refer to the two components of the doublet.
[b] Values reported with an error of ±10%.

4. Conclusions

The reversible electrochemistry observed for compounds **1** and **2** is the first example of this type of behavior for organometallic cluster complexes in water and holds out the possibility that electrochemical monitoring of cluster binding interactions with biomacromolecules is a realizable goal. The overall trends in the electrochemical data suggest that complexes that show reversible electrochemical behavior in non-aqueous solvents can be carried into water even when modified with relatively highly charged phosphine ligands. Although the electrochemistry for the remaining compounds is irreversible and complex the overall trends in the redox data reveal that the nature of the heterocycle rather than the overall charge on the complex determines the reduction potential of the water soluble cluster species. The significance of this result is that redox active cluster containing heterocyclic complexes can be designed as electrochemical probes with either positively charged water solubilizing ligands for binding to DNA [8] or with negatively charged ligands for binding to proteins with basic amino acids on their surface.

The significance of the reported changes in T_1 of the hydride resonance on binding to albumin demonstrates that this NMR resonance which is completely separated from those associated with biomacromolecules can be used as a qualitative screen for cluster bio-macromolecule interactions and that the direction of this change is understandable in terms of the expected protein – cluster electrostatic interactions. Thus, that the negatively charged clusters appear to bind more tightly than their positive analogues is not surprising in light of the fact that albumin is rich in positively charged amino acids

[16]. The combination of reversible redox behavior, direct visualization with electron microscopy and the availability of a readily observable NMR probe (the chemically inert hydride) promises to make the class of clusters reported here unique tools for probing the structure and behavior of a wide range of bio-macromolecules. What needs to be done now is to develop electrochemically active clusters that have high binding constants to specific amino acid or nucleic acid residues. This will require developing cluster functional groups and tethers that have specific and perhaps covalent interactions with given nucleic acid or peptide sequences. These studies are underway in our laboratories.

Acknowledgements

We gratefully acknowledge the support of the DOE for an EPSCOR Implementation Grant for support of this research (E.R., F.S. and D.R.), the NSF EPSCOR program for visiting scholar grants (C.N. and R.G.) and the NIH BRIN program for faculty travel award (E.R.). We also acknowledge the Italian MURST for a COFIN 2000 Grant.

References

[1] K.E. Erkkila, D.T. Odom, J.K. Barton, Chem. Rev. 99 (1999) 2777.
[2] C.J. Burrows, J.G. Muller, Chem. Rev. 98 (1998) 1109.
[3] M.J. Abedin, B. Bergman, R. Holmquist, R. Smith, E. Rosenberg, J. Ciurash, K.I. Hardcastle, J. Roe, V. Vazquez, C. Roe, S.E. Kabir, B. Roy, S. Alam, K.A. Azam, Coord. Chem. Rev. 190–192 (1999) 975.
[4] E. Rosenberg, M.J. Abedin, D. Rokhsana, D. Osella, L. Milone, N. Nervi, J. Fiedler, Inorg. Chim. Acta 300–302 (2000) 769.
[5] N. Nervi, R. Gobetto, L. Milone, A. Viale, E. Rosenberg, D. Rokhsana, J. Fiedler, Chem. Eur. J. 9 (2003) 5749.
[6] E. Rosenberg, D. Rokhsana, N. Nervi, R. Gobetto, L. Milone, A. Viale, J. Fiedler, M.A. Botavina, Organometallics 23 (2004) 215.
[7] M.P. Brown, P.A.S. Dolby, M.M. Harding, A.J. Mathews, A.K. Smith, D. Osella, M. Arbrun, R. Gobetto, J. Chem. Soc., Dalton Trans. (1993) 827.
[8] E. Rosenberg, F. Spada, K. Sugden, B. Martin, L. Milone, R. Gobetto, A. Viale, J. Fiedler, J. Organomet. Chem. 668 (1–2) (2003) 51.
[9] E. Rosenberg, F. Spada, K. Sugden, B. Martin (to be published).
[10] J. Heyrovsky, J. Kuta, Principles of Polarography, Czech Acad. Sci., Prague, 1965, p. 161.
[11] A.A. Lcek, in: A. Cotton (Ed.), Polarographic Behavior of Coordination Compounds, Progress in Inorg. Chem., vol. 5, Interscience, 1963, p. 274.
[12] H. Lund, M.M. Braizer, Organic Electrochemistry, third ed., Mercel Decker, New York, 1991, p. 732.
[13] R.K. Haris, Nuclear Magnetic Resonance Spectroscopy, Pitman, London, 1983.
[14] J. March, Advance Organic Chemistry: Reaction Mechanisms and Structure, Wiely, New York, 1985.
[15] S. Aime, W. Dastru', R. Gobetto, A. Viale, in: M. Peruzzini, R. Poli (Eds.), Recent Advances in Hydride Chemistry, Elsevier, Amsterdam, 2001, p. 351.
[16] T. Peters, All about Albumin: Biochemistry, Genetics and Medical Applications, Academic Press, New York, 1995.